VIRUS EVOLUTION

Virus Evolution, 2025, **11(1)**, veaf085
DOI: https://doi.org/10.1093/ve/veaf085
Advance Access Publication 31 October 2025
Research Article

Persistence, spillover, and evolution of co-occurring lineages of lymphocytic choriomeningitis virus

Calvin Mehl[1,2,*], Olayide Abraham Adeyemi[1], Fiona Joana Möhrer[1], Claudia Wylezich[3,4], Sven Sander[4], Katja Schmidt[5], Christina Geiger[6], Nicole Schauerte[6], Stephanie Wurr[7], Kerstin Mätz-Rensing[8], Anne Nesseler[9], Thomas Anton von Graffenried[10], Andrew Parker Morgan[11], Lisa Oestereich[2,7], Stephan Günther[2,7], Martin Beer[3], Claudia Klein[12], Dániel Cadar[7], Romy Kerber[7], Dirk Höper[3], Sven Reiche[4], Gerald Heckel[10], Rainer G. Ulrich[1,2]

[1]Institute of Novel and Emerging Infectious Diseases, Friedrich-Loeffler-Institut (FLI), Südufer 10, Greifswald–Insel Riems 17493, Germany
[2]German Center for Infection Research, Partner site Hamburg–Lübeck–Borstel–Riems, Südufer 10, Greifswald–Insel Riems 17493, Germany
[3]Institute of Diagnostic Virology, Friedrich-Loeffler-Institut, Südufer 10, Greifswald–Insel Riems 17493, Germany
[4]Department of Experimental Animal Facilities and Biorisk Management, Friedrich-Loeffler-Institut, Südufer 10, Greifswald–Insel Riems 17493, Germany
[5]Microbiological Diagnostics, German Cancer Research Center, Im Neuenheimer Feld 280, Heidelberg 69120, Germany
[6]Zoo Frankfurt, Bernhard-Grzimek-Allee 1, Frankfurt 60316, Germany
[7]Bernhard Nocht Institute for Tropical Medicine (BNITM), Bernhard-Nocht-Straße 74, Hamburg 20359, Germany
[8]German Primate Center, Leibniz Institute for Primate Research, Kellnerweg 4, Göttingen 37077, Germany
[9]Pathology & Parasitology, Landeslabor Hessen, Schubertstraße 60, Giessen 35392, Germany
[10]Institute of Ecology and Evolution, University of Bern, Baltzerstrasse 6, Bern 3012, Switzerland
[11]Department of Medicine, University of North Carolina, 101 Manning Drive CB#7085, Chapel Hill NC 27599, United States
[12]Institute of Farm Animal Genetics, Friedrich-Loeffler-Institut, Höltystr. 10, Neustadt 31535, Germany

*Corresponding authors. Calvin Mehl, Institute of Novel and Emerging Infectious Diseases, Friedrich-Loeffler-Institut, Südufer 10, Greifswald–Insel Riems 17493, Germany. E-mail: calvin.mehl@fli.de; Rainer G. Ulrich, Institute of Novel and Emerging Infectious Diseases, Friedrich-Loeffler-Institut, Südufer 10, Greifswald–Insel Riems 17493, Germany. E-mail: rainer.ulrich@fli.de

Abstract

Lymphocytic choriomeningitis virus (LCMV) is a neglected zoonotic arenavirus primarily transmitted by house mice (*Mus musculus*). In humans, LCMV infection can cause encephalitis, meningitis, or severe birth defects. In New World (NW) primates, LCMV causes acute and fatal callitrichid hepatitis (CH). We detected a continuous occurrence of LCMV lineages I and II in the house mouse population of a zoo, with the first occurrence of lineage II in 2014 and lineage I in 2021. Although the total LCMV RNA prevalence tended to increase between 2021 and 2023, this was primarily associated with lineage I, while the occurrence of lineage II tended to decrease. Despite both lineages I and II being present in house mice in the same building where NW primates are housed, only lineage II was detected in NW primates with CH, and a wild wood mouse (*Apodemus sylvaticus*). Genomic assignment detected exclusively *M.m. domesticus* ancestry in the house mouse population of the zoo, in keeping with a natural origin of house mice from the study region. Therefore, the origin of lineage I is most likely explained by the occurrence of this house mouse subspecies. The origin and incursion mode of lineage II still remain elusive. The detection of three or four LCMV genome segments in several house mice was interpreted as LCMV co-infections, and the emergence of a reassortant virus containing an S-segment of lineage II and an L-segment of lineage I. Full genome sequences showed limited diversity of the 2014 LCMV sequences from NW primates, consistent with a recent introduction of lineage II. LCMV sequences from 2021 to 2023 diverged, not only from those from 2014 but also from each other, which suggests long-term evolution in a large host population and/or potential repeated introductions of LCMV lineage II. In conclusion, the presence of two LCMV lineages within the house mouse population of the zoological garden not only poses a potential health threat for employees and visitors of the zoological garden, and potentially other zoo animals, but also provides a unique opportunity to advance our understanding of arenavirus evolution.

Keywords: LCMV; evolution; house mouse; primates; reassortment; co-infection; callitrichid hepatitis; prevalence

Introduction

Lymphocytic choriomeningitis virus (LCMV, species *Mammarenavirus choriomeningitidis*) is the only globally distributed mammalian arenavirus due to the ubiquitous distribution of its primary reservoir host, the house mouse (*Mus musculus*). Outbreaks of LCMV in Germany (Ackermann et al. 1972; Ackermann et al. 1974; Ackermann et al. 1975) and the USA (Gregg 1975; Biggar et al. 1975) have also been linked to pet Syrian golden hamsters (*Mesocricetus auratus*). Human LCMV infection may present with a range of symptoms in immunocompetent individuals, including nonspecific self-limiting flu-like illness, encephalitis, and meningitis (Ackermann et al. 1972). However, it may be particularly severe in immunocompromised individuals, such as solid organ transplant recipients (MacNeil et al. 2012; Palacios

et al. 2008). Vertical transmission has been demonstrated to have significant teratogenic effects (Barton et al. 1995), including hydrocephaly, microcephaly, epilepsy, hearing impairment, and blindness in humans (Ackermann et al. 1974; Goldwater 2021; Bonthius et al. 2007; Bonthius 2024).

In addition, LCMV was recognized as the etiological agent responsible for callitrichid hepatitis (CH) (Montali et al. 1989), a lethal infection presenting with lesions in the liver, brain, and lymphoid tissue in New World (NW) primates (Asper et al. 2001). Transmission to NW primates typically occurs *via* the oral and intragastric route (Rai et al. 1997) when consuming infected wild or feeder mice (Leong et al. 2004). Since LCMV-reactive antibodies have not been detected in wild NW primates, CH is considered a continued threat primarily to captive individuals in zoological gardens and parks (Scanga et al. 1993). Outbreaks of CH in zoological gardens may also be associated with infection in animal keepers who are often in close contact with these captive animals and their (potentially) contaminated enclosures (Montali et al. 1993; Scanga et al. 1993).

In pregnant house mice infected with LCMV, the virus is passed to the embryo, resulting in either the death and resorption of the embryo or the survival of an immune-tolerant animal that is persistently and asymptomatically infected, and sheds the virus throughout its life (Traub 1960; Bonthius and Perlman 2007). Horizontal post-natal transmission of LCMV in house mice may result in either death of the host or viral clearance and subsequent immunity (Delves 1998). Between house mice, the virus is readily transmitted through contact with the secretions or excreta of infected individuals (Skinner and Knight 1973). The risk of transmission within house mouse populations is significantly increased during close-contact behaviour such as coitus and fighting (Skinner and Knight 1973).

LCMV has a bisegmented single-stranded RNA genome with an ambisense coding strategy (Meyer et al. 2002). The small (S-) segment of ∼3400 nucleotides (nt) encodes the nucleoprotein (NP) and the glycoprotein precursor (GPC), and the large (L-) segment of ∼7200 nt encodes the Z protein (ZP) and the L protein (LP, RNA-directed RNA polymerase) (Albariño et al. 2010; Emonet et al. 2006). Five phylogenetic lineages of LCMV, numbered I–V, have been described. Lineages I and II are the most commonly detected worldwide (Albariño et al. 2010; Fornůsková et al. 2021). Lineage III comprises a single sequence from a human patient in the USA (Bullock and Meier 1984). Lineages IV and V have thus far only been found in wood mice (*Apodemus sylvaticus*) from Spain (Ledesma et al. 2009) and Germany (Mehl et al. 2024a), respectively.

Recently, the occurrences of LCMV lineages I and II were proposed to be explained by host phylogeography and/or host specificity with subspecies of house mice (Bellocq et al. 2023; Mehl et al. 2024b; Fornůsková et al. 2021). This would suggest that LCMV lineage I occurs in regions where *M.m. domesticus* (Mmd) is present, while lineage II occurs in regions inhabited by *M.m. musculus* (Mmm). However, both LCMV lineages were recently detected in Mmd from a zoological garden in western Germany, which questions the hypothesis of specificity with host subspecies (Mehl et al. 2023).

LCMV has been detected in wild house mice (Ackermann et al. 1964) and pet hamsters (Ackermann 1977; Ackermann et al. 1972) from North Rhine-Westphalia, Hesse, and other parts of western Germany going back to the 1960s. This is also the region in which CH was first reported in the zoological garden Dortmund, North Rhine-Westphalia, in 2001 (Asper et al. 2001), and where the re-emergence in 2021 was observed in Frankfurt/Main, Hesse (Mehl et al. 2023), with wild house mice implicated as the reservoir species in both studies. While only LCMV lineage I was detected in the initial CH outbreak in the zoological garden Dortmund (Asper et al. 2001), lineages I and II were found in house mice during the 2021/2022 re-emergence and lineage II in the deceased NW primate in the zoological garden Frankfurt/Main (Mehl et al. 2023).

We investigated here the persistence, spillover, and evolution of the LCMV lineages in the zoological garden Frankfurt/Main. Therefore, we aimed (i) to determine the origin of CH disease clusters in the zoological garden, (ii) to evaluate the origins and time point(s) of the emergence of LCMV lineages I and II in the study population, and (iii) to follow the occurrence and molecular evolution of each lineage.

Methods

Identification of CH cases and collection of wild house mice

As indicated in Fig. 1, we screened and typed LCMV RNA in 2009 (house mice, Mehl et al. 2023), 2014 (house mice and 9 deceased NW primates), 2021 (house mice and a deceased NW primate; Mehl et al. 2023), 2022 (house mice and wood mice; part in Mehl et al. 2023), and 2023 (house mice, Fig. 1A, a deceased NW primate, Fig. 1B, and wood mice, Fig. 1C). Additionally, other wild and captive small mammal species from 2014 and 2021–2023 were tested for LCMV RNA (Table 1). Finally, house mice collected in 2009, 2014, 2021–2023 were screened for LCMV-reactive antibodies (see Supplement for details). Table S1 provides all metadata and results of all investigations on the individual level for house mice, NW primates, and other wild and captive small mammals.

Collection of wild rodents during routine pest rodent management at the zoological garden was continued in 2022/2023. Non-target small-mammal species, as bycatch, were also investigated. The small mammals were dissected under biosafety level (BSL) 3 conditions, and the heart, lung, liver, spleen, kidneys, and brain were taken. Chest cavities were washed with 1 mL phosphate-buffered saline (PBS) for serological investigations. Wild small mammals from the zoological garden were identified morphologically or through molecular identification by sequencing a part of the mitochondrial cytochrome-*b* gene (Schlegel et al. 2012).

In 2014, nine Emperor tamarins (*Saguinus imperator*) from the zoological garden succumbed to illness. Pathology revealed acute interstitial pneumonia, acute diffuse hepatocellular degeneration of the liver, localized haemorrhages in the brain grey matter, and inflammation of the meninges, leading to the diagnoses of CH. Various tissue samples of the emperor tamarins were investigated by RT-PCR (Table 1). Additionally, for outbreak containment purposes, animals that were kept in the same or neighbouring enclosures were surveyed for signs of disease, and their LCMV infection status was determined by RT-PCR as well.

In July 2023, an additional CH case was reported in a Goeldi's monkey (*Callimico goeldii*) from the zoological garden. Based on symptoms and pathology results by the Hessian State Laboratory (Landeslabor Hessen, Giessen, Germany), selected tissue samples were sent to the Friedrich-Loeffler-Institut (FLI) for further investigation.

The exact capture location of each animal was recorded for trappings between November 2022 and November 2023.

Genomic assignment of wild house mice and a feeder house mouse

DNA was extracted from the heart tissue of the house mice using the DNeasy Blood & Tissue Kit (Qiagen, Venlo, Netherlands).

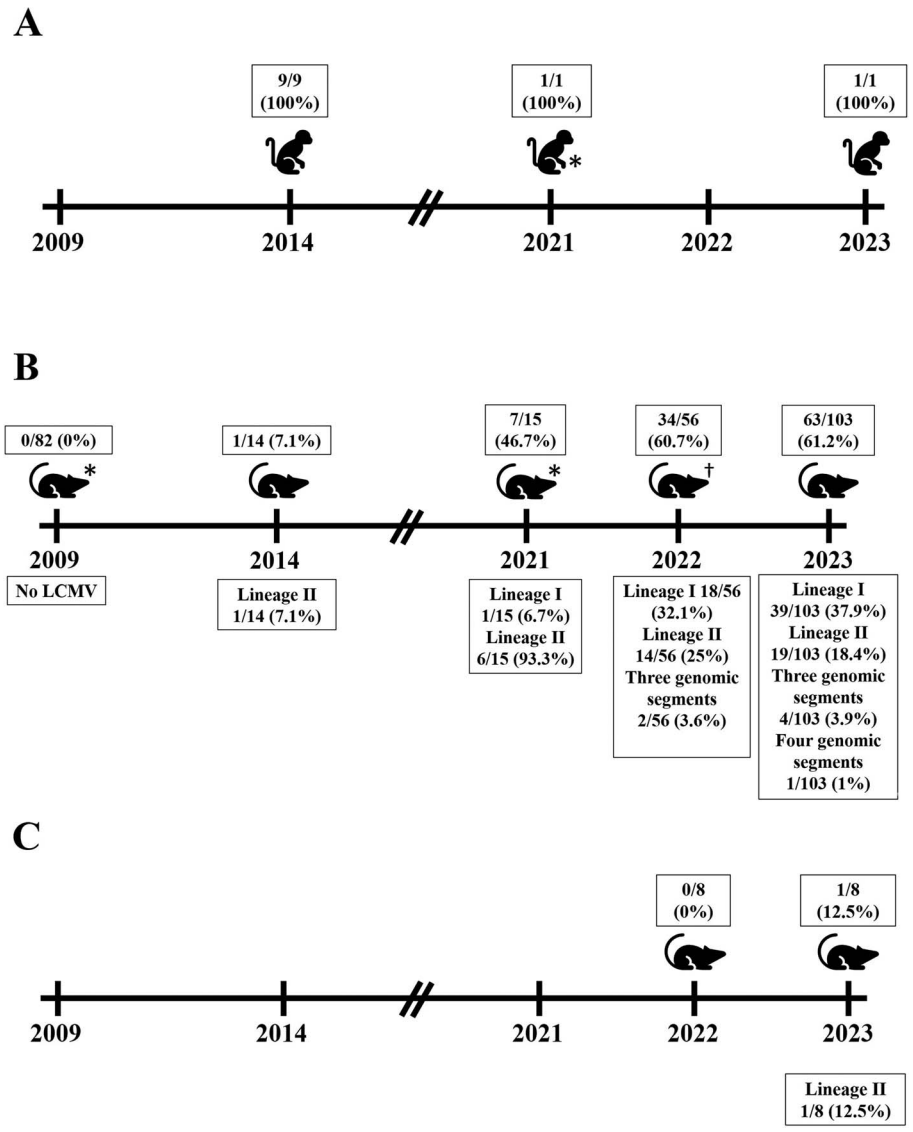

Figure 1. Timeline of LCMV RNA detection in (A) NW primates, (B) house mouse, and (C) wood mouse populations. Pictograms indicate the host species. Above the timeline, the LCMV RNA positive/total number of animals investigated is shown; below the timeline, LCMV lineage I or lineage II RNA positive/total number of animals investigated is shown; lineage I and II represent lineages of LCMV based on L-segment sequences. *Indicates data published in Mehl et al. (2023). †RT-PCR results from 35 samples previously published (Mehl et al. 2023), plus 21 new samples, of which 12 were positive from this study.

Mouse genotyping was performed using the Giga Mouse Universal Genotyping Array (GigaMUGA) (Neogen Europe, Ayr, Scotland) (Morgan et al. 2015). Genotypes were called using Illumina BeadStudio (Illumina Inc, Carlsbad, CA, USA) according to the vendor's usual procedures. A total of 24 samples were analysed: 11 collected in 2009 (7 male, 4 female) and 13 collected in 2023 (7 male, 6 female). Only samples with <15% missing calls were retained, resulting in the exclusion of one sample (KS23/066, a male collected in 2023). The resulting genotype matrix was merged with published genotypes for 807 wild house mice *M. musculus* and seven wild Algerian mice *M. spretus* (Morgan et al. 2022). After filtering for sites shared between the new and previously published datasets and removing sites with ambiguous alleles, a total of 57 839 sites (51 601 autosomal, 1708 X-linked, 17 Y-linked, 13 mitochondrial) remained for analysis.

Principal component analysis (PCA) was performed on autosomal genotypes with akt pca v.3beb346 (Arthur et al. 2017). Principal components (PCs) and single-nucleotide polymorphism (SNP) weights were first estimated from 349 putatively unrelated reference samples (Morgan et al. 2022), and the newly genotyped samples were then projected onto these PCs. Supervised ancestry analysis was performed using ADMIXTURE (Alexander et al. 2009), using 317 samples with unambiguously pure subspecies-level ancestry as reference populations and fixed $K = 3$ (that is, assuming one ancestry component per subspecies). Estimated ancestry proportions for all 23 test samples were reviewed manually.

Phylogenetic trees were inferred for Y-chromosomal and mitochondrial DNA as follows. First, a distance matrix was constructed using the Manhattan distance between haplotype vectors. Next, a tree was inferred using the neighbour-joining algorithm as implemented in the R package ape v5.5 (Paradis et al. 2004). Trees were rooted using *M. spretus* as the outgroup.

DNA extracted from the single feeder house mouse collected during 2014 was used to determine the mitochondrial d-loop sequence, following a previously described protocol (Gabriel et al. 2024).

Table 1. Prevalence of LCMV RNA and LCMV-reactive antibodies in wild and captive animals from the zoological garden

Year	Common name	Species (total number of individuals)	Tissues	Number (%) RT-PCR positive and 95% CI	Number (%) seropositive and 95% CI
2014	House mouse[a]	*Mus musculus* (*N* = 14)	Liver, brain, lung, spleen, myocardial muscle, kidney, heart fluid	1 (7.1%) 0.18–33.9	0 0–23.2
	Emperor tamarin[b]	*Saguinus imperator* (*N* = 9)	Brain, liver	9 (100%)	n.d.
	Bolivian squirrel monkey[b]	*Saimiri boliviensis boliviensis* (*N* = 1)	Liver, brain, lung, spleen, myocardial muscle, kidney, intestine, lymph nodes	0	n.d.
	Golden-bellied capuchin[b]	*Sapajus xanthosternos* (*N* = 1)	Liver, brain, lung, spleen, myocardial muscle, kidney, intestine, lymph nodes	0	n.d.
	Shrew	*Crocidura* sp. (*N* = 1)	Liver, brain, lung, spleen, myocardial muscle, kidney, heart fluid	0	n.d.
	Gundi[b]	*Ctenodactylus gundi* (*N* = 1)	Brain, organ mixture	0	n.d.
	Green acouchi	*Myoprocta pratti* (*N* = 2)	Blood, urine	0	n.d.
2021	House mouse[c]	*Mus musculus* (*N* = 15)	Brain, kidney	7 (46.7%) 21.3–73.4	1 (6.7%) 0.17–31.9
	Golden lion tamarin[b,c]	*Leontopithecus rosalia* (*N* = 1)	Brain, liver	1	n.d.
2022	Wood mouse	*Apodemus sylvaticus* (*N* = 8)	Brain, kidney	0	n.d.
	Greater white-toothed shrew	*Crocidura russula* (*N* = 1)	Brain, kidney	0	n.d.
	House mouse[d]	*Mus musculus* (*N* = 56)	Brain, kidney	34 (60.7%) 46.8–73.5	9 (16.1%) 7.6–28.3
2023	Wood mouse	*Apodemus sylvaticus* (*N* = 8)	Brain, kidney	1 (12.5%)	n.d.
	Barbary striped grass mouse[b]	*Lemniscomys barbarus* (*N* = 1)	Brain, kidney	0	n.d.
	House mouse	*Mus musculus* (*N* = 103)	Brain, kidney	63 (61.2%) 51.1–70.6	23 (22.5%) 14.9–31.9
	Goeldi's monkey[b]	*Callimico goeldii* (*N* = 1)	Brain, liver	1	n.d.

N, total number of animals in the study; n.d., no data; CI, confidence interval. LCMV-RNA-positive tissues are underlined. [a]Includes one LCMV-negative feeder mouse. [b]Captive animals. [c]Previously published (Mehl et al. 2023). [d]RT-PCR results from 35 samples previously published (Mehl et al. 2023), plus 21 new samples, of which 12 were positive from this study.

RNA extraction and RT-PCR screening

At the Bernhard Nocht Institute for Tropical Medicine (BNITM), RNA was prepared from tissue specimens (liver, brain, lung, spleen, myocardial muscle, kidney, intestine, lymph nodes) as well as from full ethylenediaminetetraacetic acid (EDTA) blood, urine, and cardiac lavage samples from wild and captive animals from the 2014 outbreak. For this, tissue samples (50–300 mg) were first homogenized in 1 ml Dulbecco's Modified Eagle Medium (DMEM) containing 10% foetal calf serum and Lysing Matrix D in a tissue homogenizer (MPbio FastPrep-24™) followed by RNA extraction using the RTP Pathogen Kit (Invitek Diagnostics, Berlin, Germany) according to the manufacturer's instructions. RNA from heart fluid was extracted using the QIAamp Viral RNA Kit (Qiagen, Hilden, Germany) according to the manufacturer's instructions.

At the FLI, kidney or brain tissue from wild rodents and other small mammals, captive primates, and other species were homogenized, and nucleic acids were extracted using a NucleoMag® VET kit (Macherey-Nagel, Düren, Germany) on a KingFisher™ Flex Purification System (Thermo Fisher Scientific, Waltham, MA, USA). At both the FLI and BNITM, nucleic acids were screened for LCMV RNA using a conventional reverse transcription (RT)-PCR with arenavirus-specific primers targeting the L-segment (Vieth et al. 2007). RT-PCR-positive samples were then prepared for Sanger sequencing using a BigDye™ Terminator v1.1 Cycle Sequencing Kit (Applied Biosystems, Waltham, MA, USA), providing sequences of ~340 nt in length.

Lineage-specific RT-qPCRs and molecular analysis of LCMV RNA tissue distribution

Based on the high-throughput sequencing (HTS) derived complete sequences of three genome segments obtained for KS23/459 brain tissue, RT-qPCR assays were developed to identify lineage I L-segment, lineage II L-segment, and lineage II S-segment (for details, see Supplement, Table S2). These three assays were used for the screening of all house mouse samples (2009, 2021–2023). The establishment of a lineage I S-segment specific RT-qPCR was attempted, but failed (see Supplement).

For analysis of the tissue distribution and RNA load determination, RNA was extracted from equal amounts (0.05 g) of brain, heart, lung, liver, spleen, and kidney tissues (see above) from 10 house mice (2022–2023) with lineage I and seven house mice (2022–2023) with lineage II LCMV RNA. The RT-qPCRs (see Supplement) for the lineage I L-segment and lineage II S-segment were tested and shown to work for the detection of lineage-specific LCMV sequences in these 17 house mice. These RT-qPCRs were also shown to be lineage specific. The RT-qPCRs were done in duplicate and an average cycle threshold (Ct) value with standard deviation was calculated per tissue.

Virus isolation and limiting dilution approach

To confirm RT-PCR results and prove the presence of infectious virus, at BNITM, LCMV isolation was performed from the homogenized tissue of the RT-PCR-positive house mouse and three emperor tamarins from 2014 in the BSL3 laboratory.

First, cell debris was pelleted by centrifugation and the cleared homogenate was added to Vero E6 cells, subclone FM (Vero FM) (Pfefferle et al. 2009). The detection of LCMV antigen follows a standard immunofluorescence assay (IFA) protocol using an NP-specific antibody (for details, see Supplement).

Virus isolation, passaging, and limiting dilution approach at the FLI followed the workflow shown in Fig. S1. For this purpose, Vero76 cells (Collection of Cell Lines in Veterinary Virology—Riems, CCLV-RIE 0228, FLI Cell Bank) were used. The LCMV antigen detection was also based on IFA but using another anti-NP antibody (for details, see Supplement).

High-throughput sequencing

Based on sequences obtained above, tissue-derived RNA of 12 house mice, one wood mouse, all 11 NW primates, and six (original isolate, plus five isolates from limiting dilution) cell culture supernatants of inoculated Vero76 cells with LCMV antigen detection were selected for HTS. Library preparation and HTS of five emperor tamarins and one house mouse from 2014 were performed as previously published (Eibach et al. 2019; Camprubí–Ferrer et al. 2024). For the rest of the samples, RNA was reverse-transcribed into complementary DNA (cDNA) using SuperScript IV First-Strand cDNA Synthesis System (Thermo Fisher) and NEBNext Ultra II Non-Directional RNA Second Strand Synthesis Module (New England Biolabs, Frankfurt am Main, Germany). The sonication-fragmented and purified double-stranded DNA was used for library preparation with an NEBNext Fast DNA Library Prep Set for Ion Torrent (New England Biolabs). The size-selected, purified, and quantified sequencing libraries were pooled and sequenced with an Ion Torrent S5 XL on an Ion 530 Chip with an Ion 510 & Ion 520 & Ion 530 Kit-Chef (all Thermo Fisher Scientific) and HTS was performed as previously described (Pfaff et al. 2022; Köster et al. 2024). This included four emperor tamarins from 2014; two house mice and a golden lion tamarin from 2021 (Mehl et al. 2023); five house mice, one wood mouse, and a Goeldi's monkey from 2023; and six virus isolates derived from house mouse KS23/459 tissue (Tables S3–S5). The initial detection of potential pathogen sequences contained in the datasets was done using the RIEMS taxonomic identification tool (Scheuch et al. 2015). Entire LCMV L- and S-segments were *de novo* assembled using SPAdes (version 3.13.0) (Nurk et al. 2013; Prjibelski et al. 2020) and analysed with Geneious Prime 2024.0 (https://www.geneious.com). Obtained segment sequences were verified with mapping analyses using the Genome Sequencer Software Suite (v.2.6, Roche), applying an identity threshold of 100% and minimum overlap length of reads of 80%.

Bioinformatics sequence analysis

The ClustalW algorithm in BioEdit was used to align sequences with previously published sequences (Hall 1999). JModelTest2 (Guindon and Gascuel 2003; Darriba et al. 2012) was used to determine the best-fit substitution model. For all three open reading frames (ORFs LP, NP, GPC) and partial L protein coding sequences, this was the generalized time-reversible model (GTR) with gamma distribution and some sites invariable. MrBayes v.3.2.7 (Ronquist et al. 2012) was then used to reconstruct phylogenetic trees for the complete coding nucleotide sequences of LP, NP, and GPC. This included 20 million iterations sampled every 2000 with the first 25% discarded as burn-in. Posterior probabilities were expressed as numbers between 0 and 1.

To determine the time to most recent common ancestor (TMRCA) of the LCMV lineage I and II strains from the zoological garden, full S- and L-segment sequences were analysed for their respective points of divergence. We used TempEst (v1.5.1) to determine whether the sequences showed a temporal signal (Rambaut et al. 2016). Thereafter, analyses were performed using the software packages BEAST 2.5, BEAUti, Tracer 1.7, and DensiTree (Bouckaert et al. 2019; Rambaut et al. 2018). The GTR substitution model was used with gamma distribution and some sites invariable. Markov chain Monte Carlo (MCMC) analysis was performed with 100 million iterations per run sampled every 1000—until convergence was met (500 million iterations in total), relaxed log-normal molecular clock, constant population size, and the first 25% discarded as burn-in. These settings were previously used in a similar study (Albariño et al. 2010). Alternate molecular clock calculations can be seen in Table S6. Convergence was determined by an effective sample size (ESS) > 300 and the trace graph shape.

Median-joining networks of full S- and L-segment sequences were reconstructed to represent inferred mutational relationships among LCMV lineage II detections in the zoological garden using Popart version 1.7 (Leigh and Bryant 2015) with an epsilon value of zero (Bandelt et al. 1999). Given the uncertainty around very large numbers of inferred mutational steps among single sequences in different clusters (see Results), we computed the average of pairwise sequence differences between clusters obtained from Bioedit (Hall 1999). We further computed the average genetic distance Dxy between sequence clusters with DnaSP6 version 6.12.03 (Rozas et al. 2017). The small number and little temporal spread of lineage I sequences prohibited similar analyses.

Detection of LCMV-reactive antibodies

Chest cavity transudate samples were taken from house mice in 2009 and 2021–2023 and were screened for LCMV-reactive antibodies. The assay is based on a glutathione-S-transferase (GST) capture immunosorbent assay in combination with a fluorescent bead technology (Luminex Corp., Austin, TX, USA; for details, see Supplement).

Statistical analysis

Statistical analysis of tissue distribution and viral RNA load data was performed in R software 4.4.2 (R Core Team, 2024). Shapiro–Wilk test and Levene's test were used to determine normality and homogeneity of variance. Because data were not normally distributed, a nonparametric analysis of variance (ANOVA) (Kruskal–Wallis test) and Dunn's test were used (Dinno, 2024). *P*-values < .05 were considered significant. Ninety-five percent confidence intervals were calculated in R version 4.4.2 (R core team, 2024).

Results

Timeline and patterns of LCMV detections in house mice, NW primates, and other small mammals

The chronology of the disease occurrence in NW primates, the occurrence of viral lineages in wild house mice, and spillover infections in wood mice are shown in Fig. 1. LCMV RNA was detected in NW primates deceased due to CH in 2014, 2021 (Mehl et al. 2023), and 2023 (Fig. 1A). The total RNA prevalence in house mice increased from 7.1% (CI 0.18–33.9) in 2014, to 46.7% (CI 21.3–73.4) in 2021 (Mehl et al. 2023), to 60.7% (CI 46.8–73.5) in 2022 (partially in Mehl et al. 2023) and 61.2% (CI 51.1–70.6) in 2023 (Fig. 1B; Fig. S2A). In 2022, no spillover infection to wood mice was detected, but one of eight wood mice was LCMV RNA positive in 2023 (Fig. 1C). LCMV RNA was not detected in any of the other captive or wild small mammals (Table 1). We were

unable to detect LCMV-reactive antibodies in house mice from 2009 (Table S1) or 2014 but detected LCMV-reactive antibodies in 6.7% (CI 0.17–31.9), 16.1% (CI 7.6–28.3), and 22.5% (CI 14.9–31.9) of house mice collected in 2021, 2022, and 2023, respectively (Table 1, Fig. S2B). This tendency of an increased seroprevalence between 2021 and 2023 was seen in the total prevalence (animals being LCMV RNA positive or negative) and in the LCMV RNA-negative animals (Fig. S2B).

LCMV typing, based on short L-segment sequences and/or HTS, indicated exclusively lineage II in spillover-infected and deceased NW primates in 2014, 2021 (Mehl et al. 2023), and 2023 and a wood mouse (Fig. 1A and C). In house mice, the LCMV RNA prevalence of lineage II showed a tendency to decrease from 2021 (40%; Mehl et al. 2023), 2022 (25%; partially in Mehl et al. 2023) to 2023 (18.4%; Fig. 1b and Fig. S2A). An increasing tendency was observed for LCMV RNA prevalence of lineage I in house mice with 6.7% in 2021 (Mehl et al. 2023), 32.1% in 2022 (partially in Mehl et al. 2023), to 37.9% in 2023 (Fig. 1, Fig. S2A).

Of the samples where the exact capture locations are known, the buildings housing the NW primates, nocturnal animals, great apes, and birds accounted for most of the house mice caught (Fig. S3). LCMV RNA–positive mice (both lineage I and lineage II) were captured in three buildings (Fig. S3).

A comparison of the tissue distribution of LCMV RNA in house mice did not show significant differences between the lineages I and II (Fig. S4). The brain tissue tended to have the highest relative LCMV RNA load, irrespective of the LCMV lineage detected. However, this tendency was more pronounced in house mice with lineage I.

LCMV lineage II sequences represent three distinct clusters

Haplotype networks were created from the full L- and S-segment sequences of lineage II from the zoological garden (Fig. 2). In both genome segments, sequences from 2014 formed a tight cluster while sequences from 2021 to 2023 formed two distinct clusters, each comprising sequences from mice and a monkey. Sequence types were only shared by samples from emperor tamarins, and other sequences from *S. imperator* differed by only a few substitutions. All these sequences were obtained from individuals that were housed together in 2014. The sequence from the single LCMV-positive house mouse from that year showed about twice the number of substitutions (Fig. 2). The two clusters with sequences from 2023 differed slightly more from each other (genetic distance L-segment: Dxy = 0.032; S-segment: Dxy = 0.028) than from the cluster of sequences from 2014 (maximum Dxy = 0.027). Interestingly, the cluster containing the sequence from the golden lion tamarin and two house mice from 2023 showed about twice as many substitutions between sequences compared to the two other clusters (Fig. 2).

TMRCA suggests recent LCMV incursion(s) in the zoological garden

LCMV seroprevalence was determined for house mice from 2009, considered as a historical baseline to narrow down the time of LCMV incursion. All 78 mice were negative for LCMV-reactive antibodies. The absence of LCMV-reactive antibodies in the house mouse population and LCMV RNA in 2009 and the detection of LCMV in 2014 provide a temporal window in which the virus likely entered the zoological garden. To further narrow this window, we used full L- and S-segment sequences from 14 individuals to estimate the time since sequence divergence of lineage II. These sequences showed sufficient temporal signal for molecular clock analyses (Fig. S5). For the L- and S-segments, x-intercepts of 2013.1 and 2012.9 were calculated, respectively (Fig. S5). Additionally, convergence (ESS > 300) was obtained for lineage II sequences from the zoological garden and the TMRCA was estimated at (mean and standard deviation) 10.4 ± 1.3 years and 12 ± 2.2 years before 2023 for the L-segment and S-segment, respectively (Fig. S6, alternative clock model results are shown in Table S6). Together, this suggests that LCMV lineage II entered the zoological garden around 2013, shortly before the first CH outbreak. The number of full sequences (L-segment $N = 8$, S-segment $N = 4$), and low sequence variability, for lineage I were insufficient to estimate when this virus entered the zoological garden.

The house mouse population in the zoological garden belongs to the Mmd subspecies

We used genomic and mitochondrial DNA from wild house mice sampled in 2009 and 2023 and the feeder mouse from 2014 to determine whether differences existed between these mice. This would tell us if these mice belonged to the naturally occurring subspecies Mmd or if indications exist for the replacement or interbreeding with Mmm that might have led to the introduction of LCMV lineage II. All tested mice had essentially pure Mmd ancestry for autosomal, Y-chromosome, and mitochondrial DNA SNPs and did not show any evidence that would suggest a replacement or hybridization. In PCA on autosomal genotypes, all individuals projected in the same cluster as Mmd specimens (Fig. 3) trapped in southern Belgium and southwestern Germany. They also carried Mmd mitochondrial DNA (Fig. S7A) and, for males, an Mmd Y-chromosome (Fig. S7B). In supervised ADMIXTURE (Alexander et al. 2009) analysis using reference populations shown in Fig. 3, the proportion of non-*domesticus* ancestry is statistically indistinguishable from zero in all individuals tested (not shown). Mitochondrial d-loop sequence from the feeder mouse (2014) clustered with Mmd, and with the other house mice from the zoological garden (Fig. S8).

Co-occurrence of lineages I and II in house mice resulted in co-infections and emergence of a reassortant virus

Phylogenetic analysis of partial L-segment sequences confirmed the presence of two LCMV lineages in some house mouse samples from 2021 to 2023 (Fig. S9). Following the workflow given in Fig. 4, the co-detection of three or four genome segments within the same brain sample of house mice emerged in 2022/2023. Seven house mice had multiple copies of the L and/or S-segments from lineages I and II (Table S3, Fig. 5). In the brain sample of house mouse KS23/445, we detected two S- and two L-segments, indicative of a co-infection of both LCMV lineages (Fig. 5, Tables S3 and S4). Furthermore, in six animals (KS23/448, KS23/449, KS23/459, KS23/460, KS23/475, and KS23/482) we detected two L-segments (lineage I and II) and one S-segment (lineage II) (Tables S3 and S4, Fig. 5). This suggests the presence of either a trisegmented virus or the co-infection of a lineage II virus and a reassortant of lineage I L-segment and lineage II S-segment. To differentiate between these options, virus isolation combined with limiting dilution was performed to separate individual viruses originating from KS23/459 brain tissue (see Supplement for details; Figs S1 and S10; Table S5). This resulted in 37 isolates containing lineage II L- and S-segments and one that contained all three genome segments present in the original tissue sample. Three isolates contained only lineage I L-segment and lineage II S-segment. Repeating the limiting dilution with the same starting material resulted in 1 isolate containing all three segments, three

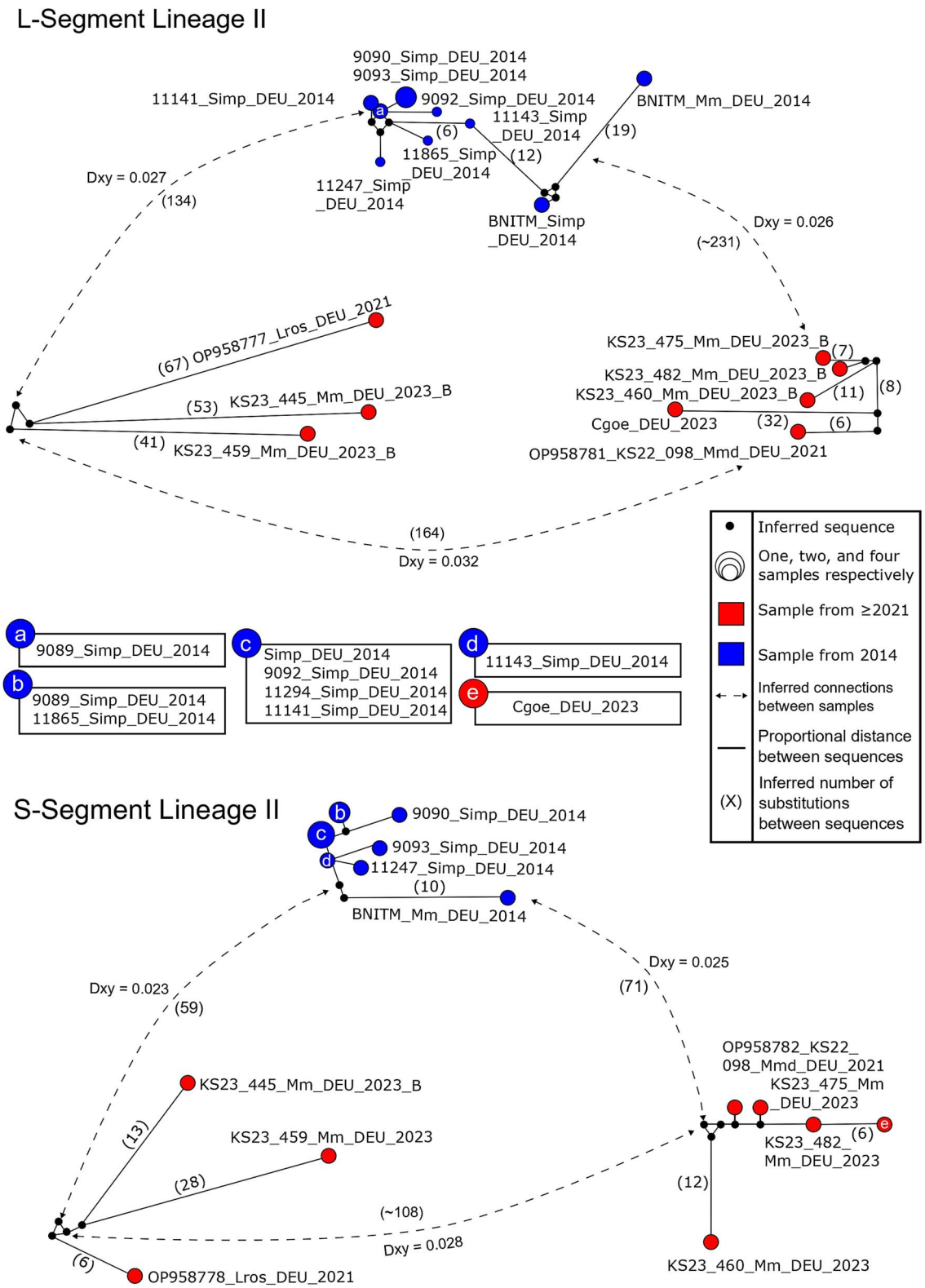

Figure 2. Median-joining haplotype networks based on the L- and S-segments of LCMV lineage II from wild house mice and New World primates from the zoological garden. Circle sizes are proportional to the number of individuals with the same sequence type. Sample identifiers are as in Fig. 5. Inferred sequences are represented with black circles. Substitutions > 5 are represented as numbers in brackets. Solid lines represent the proportional substitution distances between sequences. Dashed lines represent the inferred substitution distances between clusters (not drawn to scale). Numbers with a tilde represent the mean substitutions between clusters. Dxy represents the average genetic distance between sequence clusters. Samples from 2014 are shown in blue, samples in red were sampled in 2021–2023. Lros = *Leontopithecus rosalia*; Simp = *Saguinus imperator*; Cgoe = *Callimico goeldii*; Mm = *Mus musculus*; Mmd = *M. musculus domesticus*; DEU = Germany. A and B designate multiple sequences detected in the same sample.

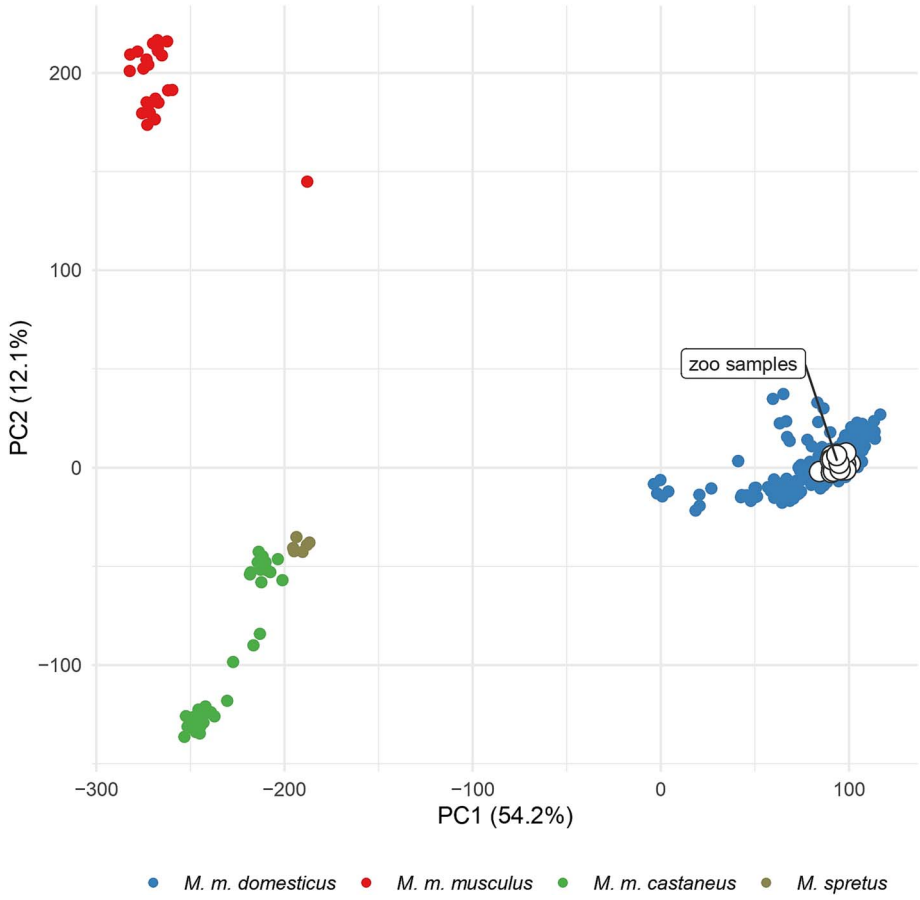

Figure 3. Ancestry of infected and noninfected wild house mice from the zoological garden determined by principal component analysis (PCA) on autosomal genotypes for 23 mice of interest (open points) plus 349 reference individuals (closed points) collected from across the geographic ranges of *Mus musculus domesticus*, *M.m. musculus*, *M.m. castaneus*, and the outgroup species *M. spretus*. Points are coloured by subspecies of origin.

containing lineage I L-segment and lineage II S-segment, and 66 containing lineage II L- and S-segments. A final sequencing of all these five KS23/459-derived isolates and its comparison to the original tissue resulted in the identification of a few synonymous nucleotide exchanges and a single nonsynonymous nucleotide exchange (His1641Tyr) in the LP coding region of the reassortant isolates (Fig. S11). Interestingly, the majority of synonymous exchanges occurred in the three reassortant isolates, in the regions coding for the N-termini of LP, NP, and GPC.

Discussion

Continuing LCMV presence in the house mouse population

The investigations suggest a continuous presence of LCMV RNA in the wild house mouse population in the zoological garden during 2014–2023. Although only lineage II RNA was detected in a single pest house mouse in 2014, both lineages I and II were detected in 2021–2023. The tendency of an increased LCMV RNA prevalence in the house mouse population during 2021–2023 was associated with the increasing RNA prevalence of LCMV lineage I, while the RNA prevalence for lineage II was decreasing at the same time. Lineage I RNA was detected in two of six pregnant mice, and at least one lineage I segment was detected in five of six lactating females, whereas no LCMV lineage II RNA was detected in pregnant animals, and in lactating animals, three of six had at least one lineage II segment of LCMV. The LCMV seroprevalence increased in the same timeframe; however, the number of house mice that were both RNA and antibody positive was quite low. Because chest cavity fluid was used, this further dilutes the whole blood and may result in an increased chance of false negatives.

The increasing RNA prevalence in the house mouse population is likely attributable to the transmission routes of LCMV and the subsequent impact of an LCMV infection on population immunity, as reflected here in the exclusively or more frequent detection of LCMV RNA lineage I in pregnant and lactating females. The vertical transmission of LCMV during pregnancy results in either the death of the mouse embryo or immune tolerance (no immune response) and persistent asymptomatic infection with continued virus shedding throughout the animal's life (Traub 1960; Bonthius and Perlman 2007). Therefore, all surviving embryos from an infected pregnant mouse will be immune tolerant and persistently infected and continuously shed the virus (Traub 1960; Bonthius and Perlman 2007). However, the observed tendency for seroprevalence to increase in RNA-negative house mice suggests an increase in horizontal transmission and subsequent seroconversion and immunity. On the other hand, the detection of LCMV RNA in lactating females indicates a likely vertical transmission and therefore may increase the prevalence in the overall population. The detection of multiple genome segments in lactating females may provide further insight into the passaging and persistence of viral reassortants during vertical transmission. It is currently not yet known whether a single strain, multiple strains, or reassortants are vertically transmitted from a coinfected mother to the offspring or how this vertical passaging is driven by evolutionary

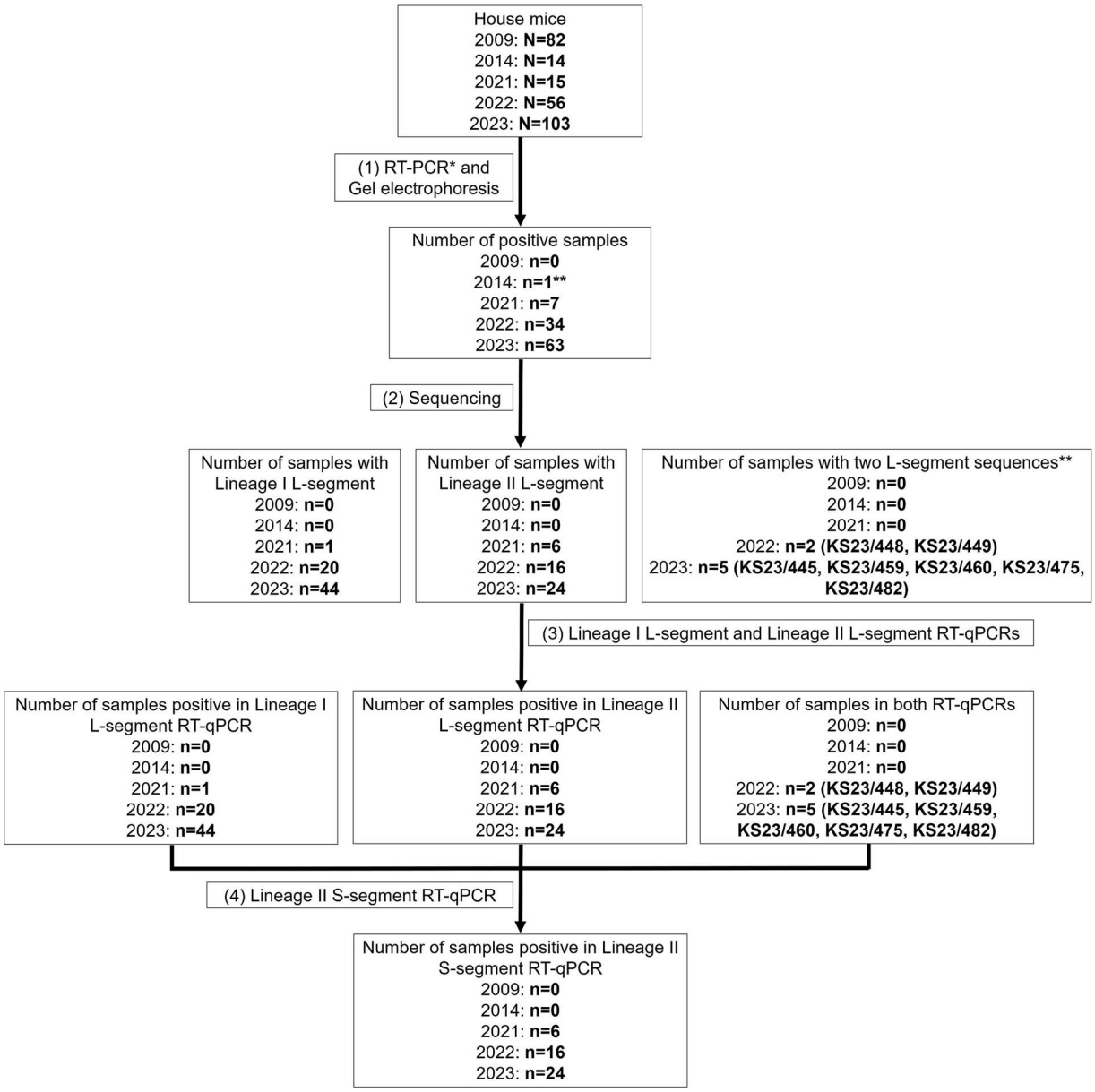

Figure 4. Workflow and results for the LCMV RT-PCR screening of house mice from the zoological garden. (1) RNA extracted from all house mouse kidney and brain samples was screened by conventional L-segment-specific RT-PCR assays (Vieth et al., 2007). (2) All positive samples were subjected to Sanger sequencing. *The conventional RT-PCR used degenerate primers. Therefore, each sample was sequenced five times (for details, see Supplement). **Sample screened at BNITM was not subjected to further RT-qPCRs. (3) All L-segment positive samples were subjected to lineage I and II L-segment RT-qPCRs (developed here). Differences in total RNA-positive animals, and the combined number of lineage I and lineage II L-segment RT-qPCR positives is due to the presence of two L-segments in some samples. (4) To determine whether two S-segments were present in these samples, all positive samples were subjected to a lineage II S-segment RT-qPCR (developed here); we failed to establish a lineage I S-segment-specific assay (see details in Supplement). *N* = total number of samples; *n* = number of samples tested positive.

constraints and/or bottleneck events. These important scientific questions need to be answered by experimental studies using lineage I, lineage II, or reassortant virus isolates.

Spillover infections in NW primates and other mammals

The detection of LCMV lineage II RNA in nine emperor tamarins from 2014 and a Goeldi's monkey from 2023 was consistent with the detection of lineage II in the CH case reported previously (Mehl et al. 2023). Despite other mammal species being kept in the same building as the NW primates, none of these other species exhibited symptoms of infection. Signs of disease caused by LCMV have only been observed in humans, NW primates, rhesus macaques (*Macaca mulatta*) (Lukashevich et al. 2003; Lukashevich et al. 2002; Zapata et al. 2011), mice, rats, and guinea pigs (Rigby 1976). Therefore, the absence of disease in these other animal species suggests they are either not susceptible to the virus or do not become ill after infection. Despite both lineage I and II being detected in wild house mice from these buildings, only lineage II was found in spillover infections in NW primates and a wood mouse. This may suggest a difference in spillover potential between these lineages or an increased susceptibility of nonhost species to lineage II, but this speculation needs further evidence from continued field studies in the zoo, accompanied by experimental studies using

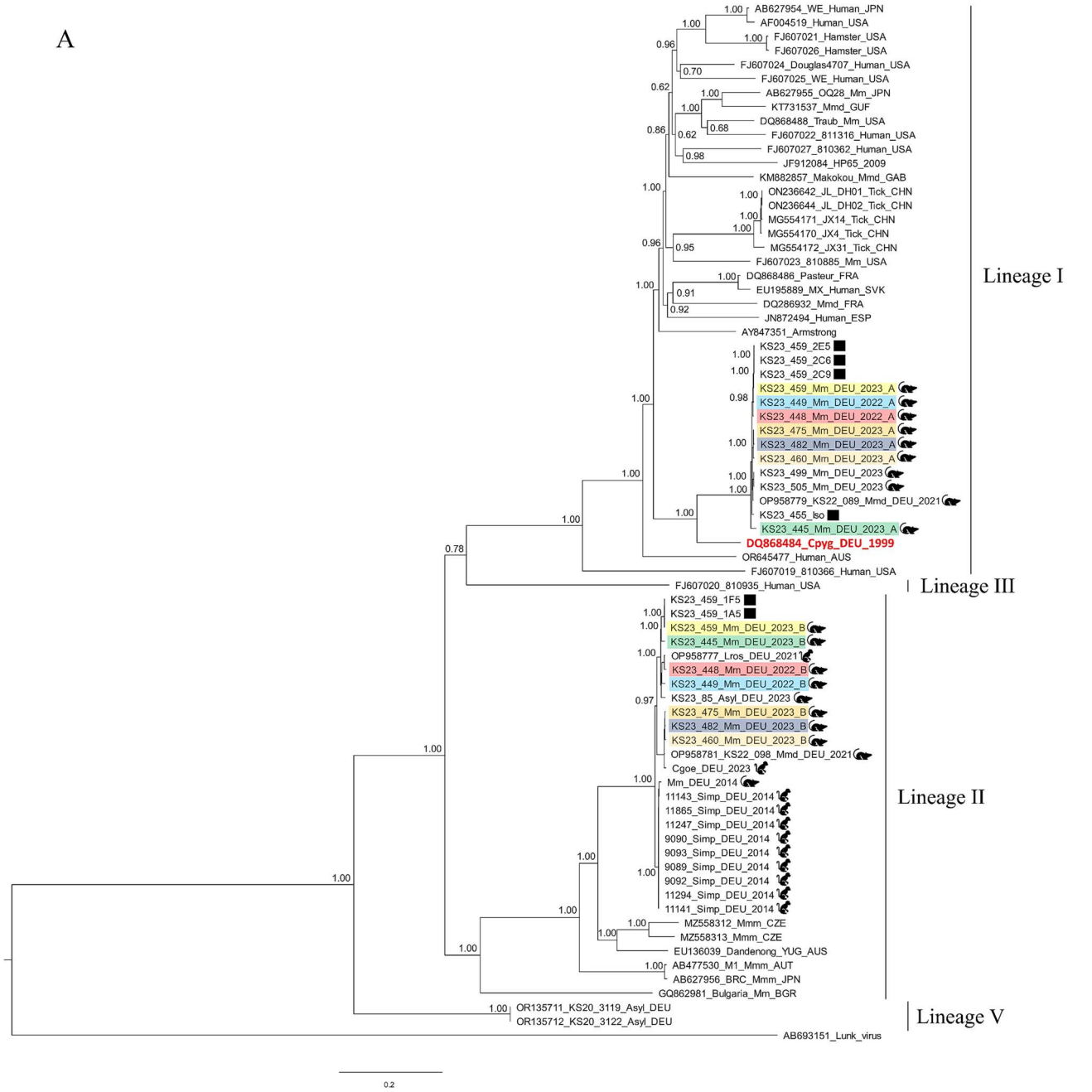

Figure 5. Phylogenetic reconstruction of the (A) L protein, (B) nucleoprotein, and (C) glycoprotein precursor complete coding regions of lymphocytic choriomeningitis virus based on nucleotide sequence alignments. Posterior probabilities > 0.6 are shown. Sample names represent: GenBank accession number, strain name, host species, country of origin (if known), year, and multiple sequences per sample were designated A and B; sequences of the same colour indicate co-detected sequences in a single sample. The lineage I sequences from zoo Dortmund (Asper et al., 2001) are shown in red and bold. Lunk virus was used as an outgroup. Scale bar indicates nucleotide substitutions per site. Squares denote sequences from isolates. Pictograms indicate the host. AUT = Austria, AUS = Australia; BGR = Bulgaria; CHN = China; CZE = Czech Republic; DEU = Germany; ESP = Spain; FRA = France; GAB = Gabon; GUF = French Guiana; JPN = Japan; SVK = Slovakia; USA = United States of America; YUG = former Yugoslavia; Lros = *Leontopithecus rosalia*; Simp = *Saguinus imperator*; Cpyg = *Cebuella pygmaea*; Cgoe = *Callimico goeldii*; Asyl = *Apodemus sylvaticus*; Mm = *Mus musculus*; Mmd = *M. musculus domesticus*; Mmm = *M. musculus musculus*; Mmin = *Mus minutoides*.

lineage I and II isolates, and wood mouse and primate cell lines. This finding is limited to house mice collected during 2023; the exact capture location of mice within the zoological garden from 2009 to 2022 was not recorded at the time. A greater number of significant differences were observed in the tissue distribution of LCMV RNA observed in house mice infected with lineage I than in house mice infected with lineage II, which might be explained by phenotypic differences between these lineages but might also be caused by differences in the time following infection, and the route of infection.

Phylogeography versus incursion of LCMV

The absence of LCMV-reactive antibodies in house mice from 2009 further supports the previously reported absence of LCMV RNA in these animals (Mehl et al. 2023). The detection of

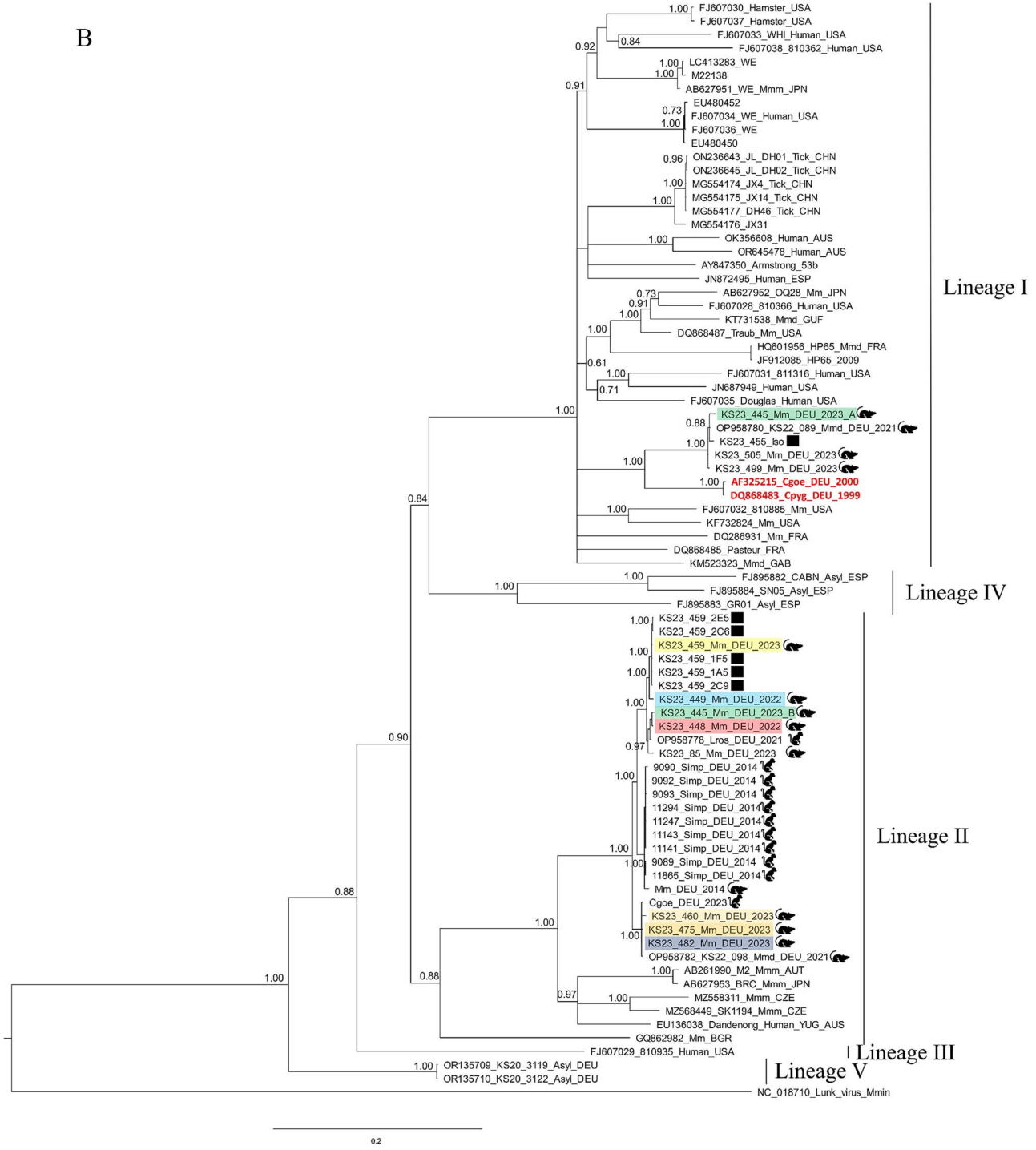

Figure 5. Continued.

lineage II LCMV in 2014 defined the window of its incursion to 2009–2014. Although the phylogenetic trees show that LCMV lineage II sequences from 2014 were closest to those from 2021 to 2023, this is relative to all published genome sequences. When examined in isolation in the haplotype networks, the separate sequence clusters are clearly evident. Our estimation of the TMRCA of the zoological garden lineage II strains was shortly before the first CH outbreak in 2014. However, these estimates are limited by the number of timepoints available and time intervals between detection of LCMV in the zoological garden (2014, 2021, 2023). This assumes a single origin to these lineage II sequences in 2014. However, we cannot exclude the additional incursion of two or more closely related strains, after 2014. Although the number of full sequences and sequence variability for lineage I were insufficient to estimate when this virus entered the zoological garden, we assume this lineage is endemic to the surrounding region of the zoological garden. This is based on the previously proposed host phylogeography (Fornůsková et al. 2021) and the detection of lineage I in a nearby zoological garden in Dortmund (Asper et al. 2001, see Fig. 5).

The tendency for RNA prevalence of lineage I to increase, and of lineage II RNA prevalence to decrease, may lend further support

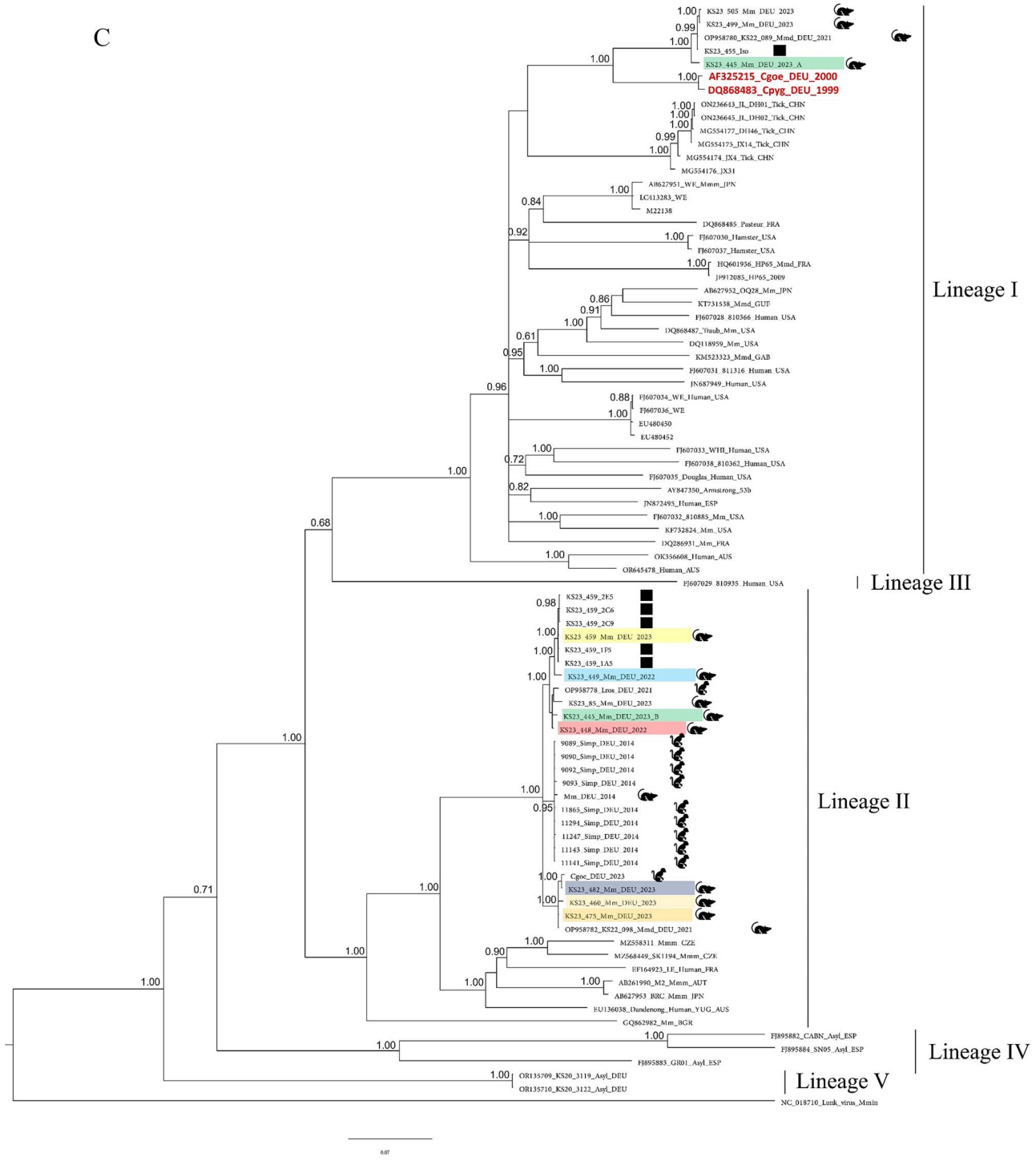

Figure 5. Continued.

for the previously proposed phylogeographical pattern. If lineage II was indeed introduced, through human intervention, to the zoological garden from an unknown source, this may explain these changes in lineage prevalence over time. Of note, the (LCMV-negative) feeder mouse from 2014 was determined to be Mmd, not giving a clue on the origin of LCMV lineage II. In addition, the zoological garden screens all incoming primates for LCMV and quarantines all incoming animals for 4 weeks, making it unlikely for the virus to have entered the zoological garden in Frankfurt/Main *via* such animals. Though Mmd is susceptible to both LCMV lineages, lineage I may have a fitness advantage in a competition situation in these hosts.

Co-occurrence and reassortment of LCMV lineages I and II

Here, we provide the first evidence of wild house mice (7 of 105) coinfected with two strains of LCMV from different lineages, indicated by the detection of three or four genome segments. However, due to limitations in creating a lineage I S-segment RT-qPCR assay, we cannot exclude the co-occurrence of lineage I and

lineage II S-segments and the presence of reassortants with the lineage I S-segment. Although arenavirus co-infections are known from snakes (Hepojoki et al. 2015), with single captive snakes being found with up to four arenavirus S-segments and eleven L-segments (Stenglein et al. 2015), this was only recently shown in mammals, with a wild single-striped grass mouse (*Lemniscomys rosalia*) from Tanzania found to be coinfected with strains of Mafiga virus (Cuypers et al. 2022).

More importantly, we detected six house mice with three LCMV genomic segments (lineage II L and S, lineage I L) and were able to show for one of these a co-infection of a lineage II strain and a genomic reassortant of lineage I L-segment and lineage II S-segment. Genomic reassortants have also been produced in Vero cell culture with Lassa virus (LASV) and Mopeia virus (MOPV), two Old World arenaviruses (Lukashevich 1992). A reassortant of LASV L-segment and MOPV S-segment showed phenotypic properties from both viruses (Lukashevich 1992). Similarly, reassortants of LCMV laboratory strains from lineage I (WE, Armstrong, and Traub) have also exhibited altered functionality compared to parental strains (Kirk et al. 1980; Riviere and Oldstone 1986).

Full genome sequences from the original tissue material were compared to those from reassortants isolated by a limiting dilution approach. Although several synonymous mutations were observed in the GPC, NP, and LP coding sequences after passaging, only a single nonsynonymous nucleotide exchange was seen in the lineage I LP encoding sequence. Whether the resulting amino acid exchange confers any phenotypic consequences is not yet known. Previous studies have also shown that passaging of LCMV may result in mutations in the GPC, NP, and LP coding regions (Grande-Pérez et al. 2002; Ruiz-Jarabo et al. 2003).

The temporal association of tendencies of increasing RNA prevalence of lineage I and decreasing RNA prevalence of lineage II, and the emergence of a lineage II S-segment/lineage I L-segment reassortant virus may suggest phenotypic differences between lineage I and lineage II viruses. Given that the L-segment encodes the viral RNA polymerase, lineage-specific molecular differences may critically affect replication efficiency, host interaction, and host specificity. In contrast, the S-segment is essential for nucleocapsid formation and immune evasion. A lineage I L-segment/lineage II S-segment reassortant is therefore likely to exhibit an altered replication phenotype. However, further data are needed to evaluate whether the epidemiological observations reflect virus intrinsic phenotype differences or are driven by ecological and host-related factors or both.

Conclusion

As recently as 2023, human LCMV infections have been reported in Hungary (Koroknai et al. 2024), and LCMV-reactive antibodies have been detected in human populations around the world (Olivieri et al. 2023), suggesting the virus still poses a threat to human health. Understanding the epidemiology and evolution of LCMV is essential to predicting potential spillover events to other species, including humans. The apparent increase of the naturally occurring LCMV lineage I versus the decrease of the likely introduced lineage II over a few years suggests a fitness advantage in the specific host and may affect spillover potential (see, e.g. Saxenhofer et al. 2019, 2022). Moreover, the first detection of multiple natural co-infections and occurrence of a reassortant lineage I/II virus, and potential phenotypic differences between these lineages, suggest a role of these processes in arenavirus evolution and host adaptation in particular. In the future, additional HTS and virus isolation attempts are necessary to determine the existence of other potential reassortants and their abundance within the reservoir population.

Acknowledgements

We would like to acknowledge the valuable help of Bernd Hoffmann, Matthias Lenk, Martin Haase, Balal Sadeghi, Simon Rohner, and Christian Reimer. We thank the zoological garden keepers and Hartmut Egdmann for performing the rodent pest control; Dörte Kaufmann, Viola C. Haring, Kira Wirtz, Max Kreutz, and Stephan Drewes for help with dissections; Patrick Zitzow, Lukas Wessler, Sabrina Bockholt, and Elisa Adam for technical assistance, and Jana Schulz for help to determine the 95% CI. We sincerely thank Alexandra Bialonski, Heike Baum, and Marike Petersen for their outstanding support and expertise in metagenomic HTS.

Author contributions

Conceptualization, C.M., S.R., R.G.U.; sample collection, C.G., N.S.; data acquisition, K.M.R., C.M., O.A.A., F.J.M., C.W., S.S., K.S., S.W., A.N., A.P.M., L.O., S.G., C.K., D.C., R.K., D.H., S.R.; data analysis, C.M., T.A.G., A.P.M., G.H.; original draft preparation, C.M.; funding acquisition, R.G.U., S.G.; critical revision, L.O., R.K., G.H., R.G.U. All authors have read and agreed to the published version of the manuscript.

Supplementary data

Supplementary data are available at *VEVOLU Journal* online.

Conflict of interest: None declared.

Funding

This work was supported by the German Center for Infection Research, Thematical Translation Unit 'Emerging Infections' (grant no. 01.808_00). Funding was received from the BMBF, grant no. 13N15449, within the PREPMEDVET project for the HTS analyses.

Data availability

All data are available within the manuscript and its Supplement Part 1, Part 2, and Part 3. The sequences were registered with the study accession number PRJEB82802. Further sequences were registered with the accession numbers PV786766-PV786777. New SNP genotypes are available on Figshare at 10.6084/m9.figshare.27857571.

Informed consent statement

Not applicable.

References

Ackermann R. Gefährdung des Menschen durch LCM-Virus-verseuchte Goldhamster. *DMW* 1977;**102**:1367–70. https://doi.org/10.1055/s-0028-1106727

Ackermann R, Bloedhorn H, Kupper B *et al.* Über die Verbreitung des Virus der lymphocytären Choriomeningitis unter den Mäusen in Westdeutschland. *Zentralbl Bakteriol Parasitenkd Infektionskr Hyg* 1964;**194**:407–30.

Ackermann R, Körver G, Turss R *et al.* Pränatale Infektion mit dem Virus der Lymphozytären Choriomeningitis. *DMW* 1974;**99**: 629–32. https://doi.org/10.1055/s-0028-1107814

Ackermann R, Stammler A, Armbruster B. Isolierung von Virus der lymphozytären Choriomeningitis aus Abrasionsmaterial nach Kontakt der Schwangeren mit einem syrischen Goldhamster (*Mesocricetus auratus*). *Infection* 1975;**3**:47–9. https://doi.org/10.1007/BF01641281

Ackermann R, Stille W, Blumenthal W *et al.* Syrische Goldhamster als Überträger von Lymphozytärer Choriomeningitis. *DMW* 1972;**97**: 1725–31. https://doi.org/10.1055/s-0028-1107638

Albariño CG, Palacios G, Khristova ML *et al.* High diversity and ancient common ancestry of lymphocytic choriomeningitis virus. *Emerg Infect Dis* 2010;**16**:1093–100. https://doi.org/10.3201/eid1607.091902

Alexander DH, Novembre J, Lange K. Fast model-based estimation of ancestry in unrelated individuals. *Genome Res* 2009;**19**:1655–64. https://doi.org/10.1101/gr.094052.109

Arthur R, Schulz-Trieglaff O, Cox AJ *et al.* AKT: ancestry and kinship toolkit. *J Bioinform* 2017;**33**:142–4. https://doi.org/10.1093/bioinformatics/btw576

Asper M, Hofmann P, Osmann C *et al.* First outbreak of callitrichid hepatitis in Germany: genetic characterization of the causative lymphocytic choriomeningitis virus strains. *Virology* 2001;**284**: 203–13. https://doi.org/10.1006/viro.2001.0909

Bandelt H, Forster P, Röhl A. Median-joining networks for inferring intraspecific phylogenies. *Mol Biol Evol* 1999;**16**:37–48. https://doi.org/10.1093/oxfordjournals.molbev.a026036

Barton LL, Peters CJ, Ksiazek TG. Lymphocytic choriomeningitis virus: an unrecognized teratogenic pathogen. *Emerg Infect Dis* 1995;**1**:152–3. https://doi.org/10.3201/eid0104.950410

de Bellocq JG, Baird SJE, Fornůskova A. Use of zoo mice in study of lymphocytic choriomeningitis Mammarenavirus, Germany. *Emerg Infect Dis* 2023;**29**:631–4. https://doi.org/10.3201/eid2903.221822

Biggar RJ, Woodall JP, Walter PD *et al.* Lymphocytic choriomeningitis outbreak associated with pet hamsters: fifty-seven cases from New York state. *JAMA* 1975;**232**:494–500. https://doi.org/10.1001/jama.1975.03250050016009

Bonthius DJ. Lymphocytic choriomeningitis virus injures the developing brain: effects and mechanisms. *Pediatr Res* 2024;**95**:551–7. https://doi.org/10.1038/s41390-023-02985-5

Bonthius DJ, Perlman S. Congenital viral infections of the brain: lessons learned from lymphocytic choriomeningitis virus in the neonatal rat. *PLoS Pathog* 2007;**3**:347–55, e149. https://doi.org/10.1371/journal.ppat.0030149

Bonthius DJ, Wright R, Tseng B *et al.* Congenital lymphocytic choriomeningitis virus infection: Spectrum of disease. *Ann Neurol* 2007;**62**:347–55. https://doi.org/10.1002/ana.21161

Bouckaert R, Vaughan TG, Barido-Sottani J *et al.* BEAST 2.5: an advanced software platform for Bayesian evolutionary analysis. *PLoS Comput Biol* 2019;**15**:Article e1006650. https://doi.org/10.5281/ZENODO.1476124

Bullock W, Meier M. Lymphocytic choriomeningitis-Georgia. *CDC-Morbid Mortal Wkly Rep* 1984;**33**:298–9.

Camprubí-Ferrer D, Tomazatos A, Balerdi-Sarasola L *et al.* Assessing viral metagenomics for the diagnosis of acute undifferentiated fever in returned travellers: a multicenter cohort study. *J Travel Med* 2024;**31**:(3). https://doi.org/10.1093/jtm/taae029

Cuypers, LN; Čížková, D, de Bellocq JG *et al.* (2022): Co-infection of mammarenaviruses in a wild mouse, Tanzania. *Virus Evol* 2022;**8**:1–5. https://doi.org/10.1093/ve/veac065

Darriba D, Taboada GL, Doallo R *et al.* jModelTest 2: more models, new heuristics and parallel computing. *Nat Methods* 2012;**9**:772. https://doi.org/10.1038/nmeth.2109

Delves PJ, Ed. *Encyclopedia of Immunology. Arenavirus, Infection and Immunity*. USA: Elsevier Ltd, Michigan, 1998.

Dinno A. Dunn.Test: Dunn's test of multiple comparisons using rank sums. 2024. R package version 1.3.6, CRAN Repos **10**:1–7.

Eibach D, Hogan B, Sarpong N *et al.* Viral metagenomics revealed novel betatorquevirus species in pediatric inpatients with encephalitis/meningoencephalitis from Ghana. *Sci Rep* 2019;**9**:2360. https://doi.org/10.1038/s41598-019-38975-z

Emonet S, Lemasson J-J, Gonzalez J-P *et al.* Phylogeny and evolution of old world arenaviruses. *Virology* 2006;**350**:251–7. https://doi.org/10.1016/j.virol.2006.01.026

Fornůsková, A, Hiadlovská, Z, Macholán, M *et al.*(2021): New perspective on the geographic distribution and evolution of lymphocytic choriomeningitis virus, Central Europe. *Emerg Infect Dis* 2021;**27**: 2638–47. https://doi.org/10.3201/eid2710.210224.

Gabriel SI, Hughes JJ, Herman JS *et al.* House mice in the Atlantic region: genetic signals of their human transport. *Genes* 2024;**15**:1645. https://doi.org/10.3390/genes15121645

Goldwater PN. A mouse zoonotic virus (LCMV): a possible candidate in the causation of SIDS. *Med Hypotheses* 2021;**158**:110735. https://doi.org/10.1016/j.mehy.2021.110735

Grande-Pérez A, Sierra S, Castro MG *et al.* Molecular indetermination in the transition to error catastrophe: systematic elimination of lymphocytic choriomeningitis virus through mutagenesis does not correlate linearly with large increases in mutant spectrum complexity. *Proc Natl Acad Sci USA* 2002;**99**:12938–43. https://doi.org/10.1073/pnas.182426999

Gregg MB. Recent outbreaks of lymphocytic choriomeningitis in the United States of America. *Bull World Health Organ* 1975;**52**:549–22.

Guindon S, Gascuel O. A simple, fast, and accurate algorithm to estimate large phylogenies by maximum likelihood. *Syst Biol* 2003;**52**: 696–704. https://doi.org/10.1080/10635150390235520

Hall. BioEdit: a user-friendly biological sequence alignment editor and analysis program for windows 95/98/NT. *Nucleic Acids Symp Ser* 1999;**41**:95–8.

Hepojoki J, Salmenperä P, Sironen T *et al.* Arenavirus coinfections are common in snakes with Boid inclusion body disease. *J Virol* 2015;**89**:8657–60. https://doi.org/10.1128/JVI.01112-15

Kirk WE, Cash P, Peters CJ *et al.* Formation and characterization of an intertypic lymphocytic choriomeningitis recombinant virus. *J Gen Virol* 1980;**51**:213–8. https://doi.org/10.1099/0022-1317-51-1-213

Koroknai A, Nagy A, Nagy O *et al.* Lymphocytic choriomeningitis virus infections in Hungary between 2017–2023—investigation of the first congenital infections. *Diagnostics* 2024;**14**:Article 1436. https://doi.org/10.3390/diagnostics14131436

Köster J, Schneider K, Höper D *et al.* Novel Pestiviruses detected in cattle interfere with bovine viral Diarrhea virus diagnostics. *Viruses* 2024;**16**:1301. https://doi.org/10.3390/v16081301

Ledesma J, Fedele CG, Carro F *et al.* Independent lineage of lymphocytic choriomeningitis virus in wood mice (*Apodemus sylvaticus*), Spain. *Emerg Infect Dis* 2009;**15**:1677–80. https://doi.org/10.3201/eid1510.090563

Leigh JW, Bryant D. PopART: full-feature software for haplotype network construction. *Methods Ecol Evol* 2015;**6**:1110–6. https://doi.org/10.1111/2041-210X.12410

Leong KM, Terrell SP, Savage A. Causes of mortality in captive cotton-top tamarins (*Saguinus oedipus*). *Zoo Biol* 2004;**23**:127–37. https://doi.org/10.1002/zoo.10121

Lukashevich IS. Generation of Reassortants between African arenaviruses. *Virology* 1992;**188**:600–5. https://doi.org/10.1016/0042-6822(92)90514-P

Lukashevich IS, Djavani M, Rodas JD *et al.* Hemorrhagic fever occurs after intravenous, but not after intragastric, inoculation of rhesus macaques with lymphocytic choriomeningitis virus. *J Med Virol* 2002;**67**:171–86. https://doi.org/10.1002/jmv.2206

Lukashevich IS, Tikhonov I, Rodas JD *et al.* Arenavirus-mediated liver pathology: acute lymphocytic choriomeningitis virus infection of rhesus macaques is characterized by high-level interleukin-6 expression and hepatocyte proliferation. *J Virol* 2003;**77**:1727–37. https://doi.org/10.1128/JVI.77.3.1727-1737.2003

MacNeil A, Ströher U, Farnon E *et al.* Solid organ transplant-associated lymphocytic choriomeningitis, United States, 2011. *Emerg Infect Dis* 2012;**18**:1256–62. https://doi.org/10.3201/eid1808.120212

Mehl C, Adeyemi OA, Wylezich C *et al.* Lymphocytic choriomeningitis virus lineage V in wood mice, Germany. *Emerg Infect Dis* 2024a;**30**:399–401. https://doi.org/10.3201/eid3002.230868

Mehl C, Wylezich C, Geiger C *et al.* Use of zoo mice in study of lymphocytic choriomeningitis Mammarenavirus, Germany (response). *Emerg Infect Dis* 2024b;**29**:631–4. https://doi.org/10.3201/eid2903.221822

Mehl C, Wylezich C, Geiger C *et al.* Reemergence of lymphocytic choriomeningitis Mammarenavirus, Germany. *Emerg Infect Dis* 2023;**29**:631–4. https://doi.org/10.3201/eid2903.221822

Meyer B, Torre J, Southern P. (2002): Arenaviruses: Genomic RNAs, transcription, and replication. In: *Arenaviruses I*, Oldstone, M.B.A. (Ed.). Berlin, Germany: Springer, 2002. https://doi.org/10.1007/978-3-642-56029-3_6.

Montali RJ, Ramsay EC, Stephensen CB *et al.* A new transmissible viral hepatitis of marmosets and tamarins. *J Infect Dis* 1989;**160**:759–65. https://doi.org/10.1093/infdis/160.5.759

Montali RJ, Scanga CA, Pernikoff D *et al.* A common-source outbreak of callitrichid hepatitis in captive tamarins and marmosets. *J Infect Dis* 1993;**167**:946–50. https://doi.org/10.1093/infdis/167.4.946

Morgan AP, Fu C-P, Kao C-Y *et al.* The mouse universal genotyping Array: from substrains to subspecies. *In G3 (Bethesda, Md)* 2015;**6**:263–79. https://doi.org/10.1534/g3.115.022087

Morgan AP, Hughes JJ, Didion JP *et al.* Population structure and inbreeding in wild house mice (*Mus musculus*) at different geographic scales. *Heredity* 2022;**129**:183–94. https://doi.org/10.1038/s41437-022-00551-z

Nurk S, Bankevich A, Antipov D *et al.* Assembling single-cell genomes and mini-metagenomes from chimeric MDA products. *J Comput Biol* 2013;**20**:714–37. https://doi.org/10.1089/cmb.2013.0084

Olivieri NR, Othman L, Flannery DD *et al.* Transmission, seroprevalence, and maternal-fetal impact of lymphocytic choriomeningitis virus. *Pediatr Res* 2023;**95**:456–63. https://doi.org/10.1038/s41390-023-02859-w

Palacios G, Druce J, Du L *et al.* A new arenavirus in a cluster of fatal transplant-associated diseases. *New Engl J Med* 2008;**358**:991–8. https://doi.org/10.1056/NEJMoa073785

Paradis E, Claude J, Strimmer K. APE: analyses of phylogenetics and evolution in R language. *Bioinformatics* 2004;**20**:289–90. https://doi.org/10.1093/bioinformatics/btg412

Pfaff F, Breithaupt A, Rubbenstroth D *et al.* Revisiting Rustrela virus: new cases of encephalitis and a solution to the capsid enigma. *Microbiol Spectr* 2022;**10**:1–13, e0010322. https://doi.org/10.1128/spectrum.00103-22

Pfefferle S, Krähling V, Ditt V *et al.* Reverse genetic characterization of the natural genomic deletion in SARS-coronavirus strain Frankfurt-1 open reading frame 7b reveals an attenuating function of the 7b protein in-vitro and in-vivo. *Virol J* 2009;**6**:131. https://doi.org/10.1186/1743-422X-6-131

Prjibelski A, Antipov D, Meleshko D *et al.* Using SPAdes de novo assembler. *Curr Protoc Bioinformatics* 2020;**70**:1–29, e102. https://doi.org/10.1002/cpbi.102

R Core Team. *R: A Language and Environment for Statistical Computing*. Vienna, Austria: R Foundation for Statistical Computing, 2024.

Rai SK, Micales BK, Wu MS *et al.* Timed appearance of lymphocytic choriomeningitis virus after gastric inoculation of mice. *Am J Pathol* 1997;**151**:633–9.

Rambaut A, Drummond AJ, Xie D *et al.* Posterior summarization in Bayesian phylogenetics using tracer 1.7. *Syst Biol* 2018;**67**:901–4. https://doi.org/10.1093/sysbio/syy032

Rambaut A, Lam TT, Max Carvalho L *et al.* Exploring the temporal structure of heterochronous sequences using TempEst (formerly path-O-gen). *Virus Evol* 2016;**2**:1–7. https://doi.org/10.1093/ve/vew007

Rigby C. Natural infections of Guinea-pigs. *Lab Anim* 1976;**10**:119–42. https://doi.org/10.1258/002367776781071503

Riviere Y, Oldstone MBA. Genetic reassortants of lymphocytic choriomeningitis virus: unexpected disease and mechanism of pathogenesis. *J Virol* 1986;**59**:363–8. https://doi.org/10.1128/jvi.59.2.363-368.1986

Ronquist F, Teslenko M, van der Mark P *et al.* MrBayes 3.2: efficient Bayesian phylogenetic inference and model choice across a large model space. *Syst Biol* 2012;**61**:539–42. https://doi.org/10.1093/sysbio/sys029

Rozas J, Ferrer-Mata A, Sánchez-DelBarrio JC *et al.* DnaSP 6: DNA sequence polymorphism analysis of large datasets. *Mol Biol Evol* 2017;**34**:3299–302. https://doi.org/10.1093/molbev/msx248

Ruiz-Jarabo CM, Ly C, Domingo E *et al.* Lethal mutagenesis of the prototypic arenavirus lymphocytic choriomeningitis virus (LCMV). *Virology* 2003;**308**:37–47. https://doi.org/10.1016/s0042-6822(02)00046-6

Saxenhofer M, Schmidt S, Ulrich RG *et al.* Secondary contact between diverged host lineages entails ecological speciation in a European hantavirus. *PLoS Biol* 2019;**17**:1–20, e3000142. https://doi.org/10.1371/journal.pbio.3000142

Saxenhofer M, Labutin A, White TA *et al.* Host genetic factors associated with the range limit of a European hantavirus. *Mol Ecol* 2022;**31**:252–65. https://doi.org/10.1111/mec.16211

Scanga CA, Holmes KV, Montali RJ. Serologic evidence of infection with lymphocytic choriomeningitis virus, the agent of callitrichid hepatitis, in primates in zoos, primate research centers, and a natural reserve. *J Zoo Wildl Med* 1993;**24**:469–74.

Scheuch M, Höper D, Beer M. RIEMS: a software pipeline for sensitive and comprehensive taxonomic classification of reads from metagenomics datasets. *BMC Bioinformatics* 2015;**16**:69. https://doi.org/10.1186/s12859-015-0503-6

Schlegel M, Ali HS, Stieger N *et al.* Molecular identification of small mammal species using novel cytochrome B gene-derived degenerated primers. *Biochem Genet* 2012;**50**:440–7. https://doi.org/10.1007/s10528-011-9487-8

Skinner HH, Knight EH. Natural routes for post-natal transmission of murine lymphocytic choriomeningitis. *Lab Anim* 1973;**7**:171–84. https://doi.org/10.1258/002367773781008597

Stenglein MD, Jacobson ER, Chang L-W *et al.* Widespread recombination, reassortment, and transmission of unbalanced compound viral genotypes in natural arenavirus infections. *PLoS Pathog* 2015;**11**:1–26, e1004900. https://doi.org/10.1371/journal.ppat.1004900

Traub E. Observations on immunological tolerance and "immunity" in mice infected congenitally with the virus of lymphocytic choriomeningitis (LCM). *Arch Virol* 1960;**10**:303–14. https://doi.org/10.1007/BF01250677

Vieth S, Drosten C, Lenz O *et al.* RT-PCR assay for detection of Lassa virus and related old world arenaviruses targeting the L gene. *Trans R Soc Trop Med Hyg* 2007;**101**:1253–64. https://doi.org/10.1016/j.trstmh.2005.03.018

Zapata JC, Pauza CD, Djavani MM *et al.* Lymphocytic choriomeningitis virus (LCMV) infection of macaques: a model for Lassa fever. *Antivir Res* 2011;**92**:125–38. https://doi.org/10.1016/j.antiviral.2011.07.015

Virus Evolution, 2025, **11**, 1–16
https://doi.org/10.1093/ve/veaf085
Research Article